Molecular Physics, 2013
Vol. 111, No. 20, 3136–3146, http://dx.doi.org/10.1080/00268976.2013.771802

RESEARCH ARTICLE

Demixing and nematic behaviour of oblate hard spherocylinders and hard spheres mixtures: Monte Carlo simulation and Parsons–Lee theory

Francisco Gámez[†], Rafael D. Acemel and Alejandro Cuetos[*]

Departamento de Sistemas Físicos, Químicos y Naturales, Universidad Pablo de Olavide, 41013 Seville, Spain

(*Received 4 December 2012; final version received 24 January 2013*)

Parsons–Lee approach is formulated for the isotropic–nematic transition in a binary mixture of oblate hard spherocylinders and hard spheres. Results for the phase coexistence and for the equation of state in both phases for fluids with different relative size and composition ranges are presented. The predicted behaviour is in agreement with Monte Carlo simulations in a qualitative fashion. The study serves to provide a rational view of how to control key aspects of the behaviour of these binary nematogenic colloidal systems. This behaviour can be tuned with an appropriate choice of the relative size and molar fractions of the depleting particles. In general, the mixture of discotic and spherical particles is stable against demixing up to very high packing fractions. We explore in detail the narrow geometrical range where demixing is predicted to be possible in the isotropic phase. The influence of molecular crowding effects on the stability of the mixture when spherical molecules are added to a system of discotic colloids is also studied.

Keywords: binary mixtures; discotics; oblate hard spherocylinder; hard sphere; Parsons–Lee, phase diagram

1. Introduction

The term self-assembly has been defined by Grzybowski and co-workers as 'the spontaneous formation of organised structures from many discrete components that interact with one another directly' [1]. This definition implies that the phenomenon consists of a spontaneous process in which individual molecules are collectively arranged in partially ordered structures through non-covalent interactions. An improved knowledge of the self-organisation features of discotic particles has given rise as a field that has attracted a huge interest due to its promising technological applications with special attention to the nanoscale [2,3]. These applications came mainly from the self-assembly in columnar structures. In the so-formed columns or nanowires the electric conductivity is almost unidirectional along the columnar axis due to the overlap between π orbitals typical in aromatic rings in real discotic molecules. This electronic behaviour is of key importance in photovoltaic and semiconductor devices or OLEDs [1,4,5]. In contrast, although interesting properties have been established [6–8], the applicability of discotic nematic phases in optoelectronics is restricted because these phases have a longer switching time in discotic particles than in their prolate counterparts [9]. Moreover, contrary to the phase diagram of rod-like particles, where the nematic phase can also appear for not very elongated particles [10,11], columnar phases are dominant in the phase diagram of oblate particles and a high shape anisotropy becomes necessary for nematic phases to be stable [12–14]. Hence, the advent of novel applications of discotic nematogens will be benefited from computational predictions about the fundamental molecular properties regarding the stability of the discotic nematic phase over a broad range of thermodynamic parameters.

Shedding light on the mesophases stability caused by the excluded volume or molecular crowding effects induced by depleting agents has been the goal of many recent investigations [15–23]. The reason that underlies these size and shape-dependent effects was described in the pioneering work of Asakura and Oosawa [24]. In this work concerning mixtures of spheres of very dissimilar sizes, an attractive depletion potential among the bigger species is demonstrated to be induced by the presence of the smaller components in the mixture. For fluids with non-spherical particles, the situation is much more complex because, besides the depletion effect typical of size asymmetry, the orientational degrees of freedom also play an important role. In these shape-dissimilar binary mixtures, the appearance of novel phases and properties that complicate and make richer the one component phase diagram and internal structure of the fluid, is widely documented [22,25–29]. In any of the above-mentioned cases, thermodynamical instability leads to the existence of demixing phenomena, where the corresponding presence of ordered phases at relatively low global density becomes possible. These effects

[*]Corresponding author. Email: acuemen@upo.es
[†]Present address: Instituto de Estructura de la Materia, CSIC, Serrano 121, E-28006 Madrid, Spain.

are also present in the theoretical frame provided by hard or athermal systems and present a fundamental interest in their own right. Besides their simplicity, hard models qualitatively account for relevant features in the behaviour of real substances [30]. From a theoretical viewpoint, hard models have been traditionally described using the ideas outlined in Onsager's pioneering work [31] – exact in the limit of infinitely thin rods – about the isotropic-to-nematic (I–N) transition.

Keeping this in mind, in this work we focus on the effect of the addition of hard spherical particles (HS) on the phase diagram of the fluid of oblate hard spherocylinder (OHSC) [12–14,32,33]. Historically, the binary mixture of spherical and disk-like particles has been studied in the small disk-like/big spherical particles limit [34–37]. In this limit the oblate particles act as depleting agent, favouring the aggregation and crystallisation of the spherical particles. The opposite limit, where the anisotropy of discotic particles is high enough to present liquid-crystalline phases and the spherical particles are smaller than the disk-like ones, has been scarcely explored [38,39] and this limit will constitute the main objective of this paper. This task has been tackled by adapting the extension of Onsager's approach proposed by Parsons–Lee (PL theory) [40,41] to the binary mixture of hard spheres and oblate hard spherocylinders (OHSC–HS fluid). This approximation has been recently applied to the study of the isotropic–nematic transition in monocomponent fluid of both discotic [42–44] and prolate particles [10] and also to the binary mixture of spherical and rod-like particles (HSC–HS fluid) [22], with good agreement between theory and simulation.

Alternatives studies based on fundamental measure theory proposed in the seminal work of Rosenfeld [45] are widely extended in the literature (see for example Refs. [46–48]). These approaches take into account spatial correlations accurately, providing a correct description of phases with positional and orientational order. The main drawbacks of these procedures is that additional assumptions should be considered to obtain tractable expressions for the free energy functionals (such as the parallel alignment restriction), and the difficult to advance in this theoretical frame keeping manageable expressions for free energy and equation of state. In contrast, the density functional-like theory of Parsons–Lee lacks of this complexity, being more intuitive and showing a great potentiality to provide an accurate and manageable description of the thermodynamic behaviour in fluids with orientational degrees of freedom.

Hence, the aim of the present work is to extend the PL approach to determine the isotropic–nematic transition and the thermodynamic behaviour in both phases. Besides, we also used this theoretical approximation to determine the conditions where the isotropic fluid is not stable against demixing. To complete this study, extensive computer simulations were carried out in order to check the theoretical predictions and to obtain further insight into the characteristics of this fluid.

Thus, the paper is arranged as follows. In Section 2, a detailed description of the implementation of the Parsons–Lee approach for the binary mixture of the OHSC–HS fluid is provided. Computer simulation details will also be described in this section. The comparison of theoretical and simulation results for the stability of the mixture against demixing in the isotropic phase as well as nematic stability and equations of state for a broad range of parameters is given in Section 3. Finally, in Section 4 we summarise and present the main conclusions of our work.

2. Methodology

2.1. Coarse grained model and Parsons–Lee theory

This work is based on the OHSC geometrical model [32]. An OHSC is the revolution body obtained by the rotation of a cylinder of length σ and width L capped with hemispheres of diameter L around a perpendicular axis centred on $\sigma/2$. As commented in the Introduction, Onsager's seminal work shows that virial expansion up to second order gives exact results in the limit of hard infinitely thin prolate spherocylinders [31]. The extension of the theory to higher densities was made by Parsons and Lee taking into account subsequent terms in the virial expansion in a non-explicit way using the hard sphere (HS) reference structure [40,41]. In both the Onsager and Parsons–Lee theories, the excluded volume effects are the parameters driving the transition. This allows us to extend Parsons–Lee approach to convex bodies whose excluded volume is known [27]. By reviewing this approach, it is understood how it is based on a decoupling of the distribution function in a radial and an orientational part $f(\Omega)$, where Ω is the solid angle that defines the orientation of the particle, assuming the radial distribution function at contact distance at a given density is independent of orientation. This radial distribution at contact is assumed to be the HS radial distribution function at contact, which is simply given by $(Z_{HS}-1)/(4v_m)$, where Z_{HS} is given by the well-known Carnahan–Starling equation of state [49]. Here $v_m = x_s v_s + x_c v_c$ is the average volume of the mixture, where v_s and v_c are the molecular volume of spherical and discotic particles. Z_{HS} depends on the packing fraction defined as $\eta = \rho v_m$. With these approximations, the Helmholtz free energy F of N particles (N_c spherocylindrical particles and N_S spheres) within a volume V at particle density $\rho = N/V$ obtained by the virial route is [10]:

$$\frac{F}{N\kappa_B T} = \frac{\Psi_0}{\kappa_B T} + \ln\rho + x_s \ln x_s + x_c \ln x_c + x_c \int d\Omega f(\Omega) \ln(4\pi f(\Omega))$$

$$+ \frac{F_{HS}^{exc}}{8v_m} \sum_{i,j} x_i x_j \int_{\Omega'} \int_{\Omega} d\Omega d\Omega' f(\Omega) \times f(\Omega') \omega_{exc}^{i,j}(\Omega, \Omega'), \quad (1)$$

where κ_B is the Boltzmann constant, $x_c = N_c/(N_c + N_s)$ the molar fraction of spherocylinders and $x_s = 1 - x_c$ is the molar fraction of hard spheres of diameter D_s. F_{HS}^{exc} is the excess free energy of HS as obtained from the Carnahan–Starling approximation [10,22]. Ψ_0 contains the contributions of the rotational and translational de Broglie wavelengths. The excluded volume terms $\omega_{exc}^{i,j}$ between particles of species i and j are given by:

$$\omega_{exc}^{s,s} = \frac{4}{3}\pi D_s^3 \quad (2)$$

for the sphere–sphere term,

$$\omega_{exc}^{s,c} = \frac{\pi}{6}\left\{L^3 + \frac{3}{4}\pi L^2(D_s - L) + \frac{3}{2}L(D_s - L)^2\right\} \quad (3)$$

for the spherocylinder–sphere term, and

$$\omega_{exc}^{c,c} = \frac{\pi}{2}\sigma^3 \sin\gamma + \pi\sigma^2 L + \pi^2 \sigma L^2 + \frac{4}{3}\pi L^3 + 2\sigma^2 L \sum_{n=0}^{\infty} -\frac{\pi^3}{8} \cdot \frac{4n+1}{(2n-1)(2n+2)} \times P_{2n}(0)^4 P_{2n}(\cos\gamma) \quad (4)$$

for the spherocylinder–spherocylinder term with normal vectors forming an angle $\gamma(\Omega, \Omega')$[50], where $P_n(x)$ denotes the nth order Legendre polynomial of argument x. The functional derivation of the free energy and subsequent minimisation with the Lagrange multiplier method allows us to obtain a compact integral equation for the orientational distribution function $f(\Omega)$,

$$\ln[4\pi f(\Omega)] = \lambda - 1 - \frac{x_c F_{HS}^{exc}}{4v_m} \int_{\Omega'} d\Omega' f(\Omega') \left[\frac{\pi}{2}\sigma^3 \sin\gamma + 2\sigma^2 L \sum_{n=0}^{\infty} -\frac{\pi^3}{8} \cdot \frac{4n+1}{(2n-1)(2n+2)} P_{2n}(0)^4 P_{2n}(\cos\gamma)\right]. \quad (5)$$

This equation has always the trivial solution $f(\Omega) = 1/4\pi$, corresponding to the isotropic phase. To obtain a nematic solution, given the centrosymmetrical geometry of the problem, the angular terms can be expanded in Fourier–Legendre series and, with the help of the addition theorem and orthogonality properties of Legendre polynomials, a handier expression can be obtain for $f(\Omega) = 2\pi f(\theta)$ [22]:

$$f(\theta) = K \exp\left[- \frac{x_c \pi F_{HS}^{exc}}{2v_m} \left(\sum_{n=0}^{\infty} \frac{\pi}{2}\sigma^3 a_{2n} d_{2n} \frac{2}{4n+1} \times P_{2n}(\cos\theta) + 2\sigma^2 L \sum_{n=0}^{\infty} -\frac{\pi^3}{8} \cdot \frac{2a_{2n}}{(2n-1)(2n+2)} P_{2n}(0)^4 P_{2n}(\cos\theta) \right) \right], \quad (6)$$

where K is a normalisation factor and a_{2n} and d_{2n} are the coefficients of the Fourier–Legendre expansion for $\sin\gamma$ and $f(\theta)$, respectively.

In order to determine the orientational distribution function that minimises the free energy for a given composition and packing fraction, Equation 6 is iteratively solved until a_n expansion coefficients converge. Once a converged solution of $f(\theta)$ is obtained, the free energy can be calculated with Equation 1. From F, the different thermodynamic quantities are calculated from the partial derivatives of the free energy. Particularly, pressure and chemical potentials are obtained by analytical derivation of F respect V, N_c and N_s at each packing fraction and composition. The coexistence between the isotropic and nematic phases is determined by equalling pressure and chemical potentials of spheres and discotic particles in both phases. This is a system of three equations with three unknown quantities: the packing fractions in both phases and the molar fraction of oblate particles in the nematic phase, while the composition of the isotropic phase is fixed as parameter. In order to ensure the consistency of the results, several numerical methods have been employed to solve this system of equations [22].

We have extended the above described methodology in order to evaluate the stability of the isotropic OHSC–HS fluid against demixing. For this purpose, the spinodal and binodal curves for the isotropic–isotropic (I–I) coexistence have been calculated. Spinodal curves delimit the region of absolute instability of a mixture. In other words, within this region, the mixture is unstable against demixing and the system suffers a phase separation. In the frame of Parsons–Lee theory, the spinodal curves can be calculated analytically with the help of the formalism proposed by van Roij and Mulder [51]. It establishes that the stability conditions for a thermodynamics state are

$$\left(\frac{\partial^2(\beta F/N)}{\partial(1/\rho)^2}\right)_x > 0, \quad (7)$$

$$\left(\frac{\partial^2(\beta F/N)}{\partial x^2}\right)_\rho > 0, \quad (8)$$

$$\left(\frac{\partial^2(\beta F/N)}{\partial(1/\rho)^2}\right)_x \cdot \left(\frac{\partial^2(\beta F/N)}{\partial x^2}\right)_\rho - \left(\frac{\partial^2(\beta F/N)}{\partial x \partial(1/\rho)}\right) > 0, \quad (9)$$

where x is the molar fraction of one of the components and $\beta = 1/\kappa_B T$. If any one of these inequalities becomes negative, the homogeneous mixing of the binary system becomes unstable and, consequently, a demixing transition is produced. Hence, the spinodal curve in a given binary mixture separates the phase diagram region where these inequalities are fulfilled from the region where any of the three inequalities is not satisfied.

Coexistences between two different isotropic phases are described by means of the calculation of the binodal curves. This condition requires the existence of two isotropic states with different packing fraction and composition in thermodynamical equilibrium. The determination of the binodal coexistence can be performed by equalling pressures and chemical potentials of the components within the same procedure followed for the calculation of the I–N coexistence, but avoiding the calculation of $f(\theta)$. Again, it is necessary to solve a system of three equations where the unknown quantities are the packing fraction in both phases and the composition of one of them.

2.2. Computer simulation details

In order to check the predictions obtained with the Parsons–Lee theory described above, a series of Monte Carlo simulations at constant number of particles, temperature and pressure has been carried out (MC–*NPT* computer simulation). These simulations were carried out for different particle sizes and compositions. To determine the Nematic-to-isotropic transition, for a given sizes/composition set, a configuration with randomly distributed particles with all the discotic particles following the same director vector was created. This artificial configuration was thermalised at a high enough pressure to obtain a equilibrated nematic state. From this state, a series of MC–*NPT* simulations with decreasing pressure were carried out. In general, long simulations have been necessary to thermalise the system at each pressure. Typically, along 5×10^5 Monte Carlo cycles for equilibration and 1×10^6 MC cycles to obtain averages were necessary at each thermodynamical state. A MC cycle consists on N attempts to displace and/or rotate (if it is an OHSC particle) a particle chosen at random plus an attempt to change the volume. The simulation was done in a system with 3000 particles. The volume changes were attempted by the independent and random change in the length of either side of the simulation box. To discriminate the nematic from the isotropic phase, the nematic order parameter was calculated with the standard procedure of diagonalisation of a symmetric tensor built with the orientation vectors of the discotic particles [52]. In the context of this study, it was also relevant to check if the system presents any kind of spatial structures typical of the columnar phases. For this reason, several distribution function described in Ref. [32] were monitored. Throughout this paper, dimensionless units were used. Hence, the diameter of the discotic particles D has been taken as length unit, and we will hereinafter refer to $L^* = L/D$ and $D_s^* = D_s/D$ as width of discotic and diameter of spherical particles, respectively. The pressure has been reduced as $P^* = \beta P D^3$. The composition of the system will be expressed with both the molar fraction of spheres x_s and the volume fraction of spheres x_v, defined as $x_v = x_s v_s / v_m$, with $v_m = x_s v_s + x_c v_c$ where v_s is the spheres' volume and v_c the volume of the discotic particles.

3. Results and discussion

3.1. Demixing in the isotropic phase: spinodal curves

We start the discussion by exploring the stability of the OHSC–HS fluid in the isotropic phase against demixing as obtained with the calculation of the spinodal curves. The spinodal is defined as the ensemble of points that separate the region where the isotropic mixture is stable or metastable from where it is unstable as already mentioned. As it was commented in the Methodology, this is determined by the fulfilment of conditions 7 to 9. In the top panel of Figure 1, the stability of the isotropic mixture in a broad range of particle sizes for the OHSC–HS fluids is sketched. In this figure, the minimum packing fraction in the spinodal curve for a given size of the particles, regardless of its composition, η_L is shown. It is easily observed from this graph that the OHSC–HS mixture is stable against demixing up to very high packing fraction. According to PL theory, only for very thin discotic and very big spherical particles the isotropic mixture becomes unstable at a moderate packing. It is relevant to point out that a region exists for $D_s \approx D$ where the isotropic OHSC–HS is not unstable for any packing fraction or composition. For more details, some typical OHSC geometries ($L^* = 0.08$, 0.1 and 0.3) are considered in bottom panel of Figure 1. In this graph, the minimum packing fraction at which Parsons–Lee formalism predicts the instability of the OHSC–HS isotropic fluid is plotted against the diameter of spherical particles. We can observe that the minimum value of the packing fraction in the spinodal curve presents three different regions for a given value of L^*. At very small spheres' diameter, there is a minimum in the packing fraction at which the instability could appear. Roughly, in this case the diameter of the spheres is close to the width of the discotic particles. This value of η_L grows very fast up to a maximum η value reached at a moderate values of D_s^* (in the range of $D_s^* \approx 0.5 - 0.7$). This maximum is displaced to larger values of D_s^* when L^* increases. This could be interpreted as the stability against demixing under any thermodynamic condition for D_s close to D in the OHSC–HS fluid. For values of D_s^* above 4, the packing fraction of the spinodal reaches a plateau roughly independent on the diameter of the spherical particles. In general, the limiting value of the

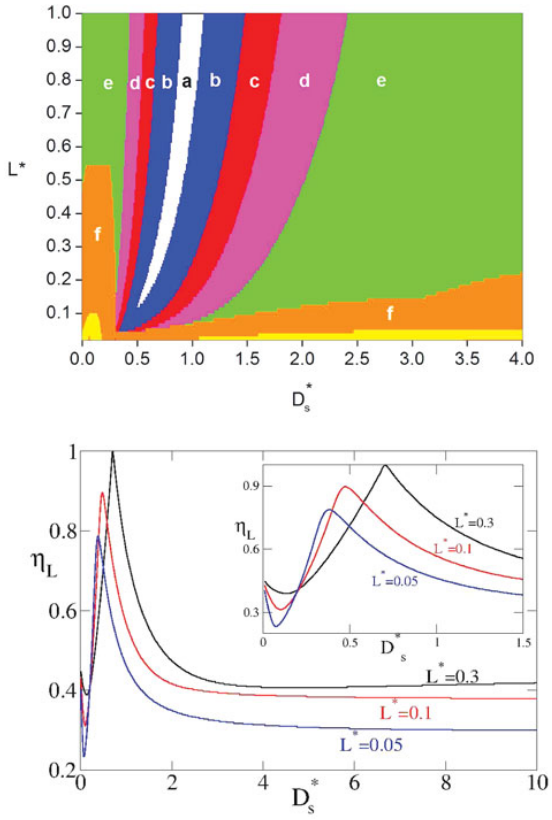

Figure 1. Top panel: Map of the stability against I–I demixing. In each region for given values of L^* and D_s^*, the value of the packing fraction at the minimum of the I–I spinodal curve is (a) $\eta_L > 0.8$; (b) $\eta_L > 0.7$; (c) $\eta_L > 0.6$; (d) $\eta_L > 0.5$; (e) $\eta_L > 0.4$; and (f) $\eta_L > 0.3$. In the rest of the graphic, $\eta_L < 0.3$. Bottom panel: Dependence of η at the minimum of the I–I spinodal curve with D_s^* at $L^* = 0.05$ (lowest curve at large D_s^*), 0.1 (intermediate curve) and 0.3 (highest curve). The region of small D_s^* is shown in the inset with more detail.

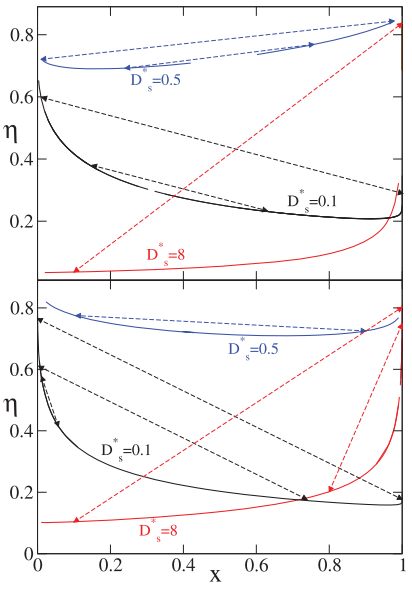

Figure 2. I–I binodals predicted by Parsons–Lee theory for the OHSC–HS fluid for $L^* = 0.05$ (top panel) and $L^* = 0.3$ (bottom panel) and $D_s^* = 0.1$ (intermediate curve at low x_v), 0.5 (upper curve at low x_v) and 8 (lower curve at low x_v). The packing fractions are represented versus x_v in the coexisting isotropic states. Tie lines joining some coexisting states are included for illustration.

packing fraction described has a positive correlation with L^*, and thus it gets higher the higher L^* does. The only exception to this general behaviour is between the minimum and the maximum described before. In this region, the opposite trend is found, and the value of η_L is higher the lower is L^*. Hence, the OHSC–HS will be stable (or metastable) up to relatively high packing fractions. In general, the values of η_L reported in both panels of Figure 1 are above the transition from the isotropic to a more ordered phase – nematic or columnar – in the monocomponent OHSC fluid [12,14,32].

In order to obtain further insight into the demixing phenomenon of the OHSC–HS fluid, we have calculated the binodal curves for the I–I coexistence in these three regions. In Figure 2, the binodals for OHSC particles with $L^* = 0.05$ (top panel) and 0.3 (bottom panel) and HS with diameters $D_s^* = 0.1$, 0.5 and 8 are shown. A few tie lines linking coexisting points have been added in order to facilitate the interpretation. Briefly, in a given I–I coexistence curve, states with low volume fraction of spheres are in coexistence with states with higher values of x_v and states with intermediate values of x_v coexisting between them. Depending on the relative size between OHSC and HS, three different behaviours can be observed as emerge from both panels of Figure 2. At low sphere diameters ($D_s^* = 0.1$), the coexistence is between high-packed states with low volume fraction of spheres and low-packed states with high volume fraction of spheres. In contrast, in fluids containing bigger spheres, the coexistence occurs between states with low packing fraction and volume fraction of spheres and dense states with high fraction of spheres. For fluids with $D_s^* = 0.5$, all the states in the binodal curve have a very high packing fraction, confirming the existence of a region where the OHSC–HS mixture is fully miscible. These different behaviours are coincident with the three regions identified in the study of spinodal curves.

Focusing in the two first cases, it can be observed that the Parsons–Lee theory developed in this work results in a well-known scenario where the smaller particles act as depleting agents, favouring the aggregation of the bigger ones. Hence, in OHSC–HS mixtures in which spheres are bigger than the OHSC, the oblate particles stand mostly in

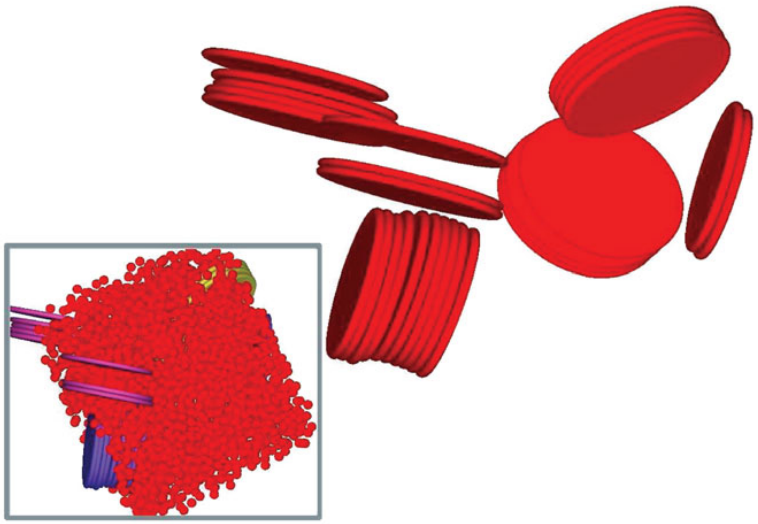

Figure 3. Snapshot of a typical configuration of a demixed state for $L^* = 0.05$ and $D_s^* = 0.1$ obtained by MC–*NPT* simulation. To facilitate the visualisation, the spheres have been removed in the main picture. In the inset all the particles are shown.

a phase at lower packing fractions. This packing fraction is, for all the values of L^*, below the transition value from the isotropic phase to a more ordered phase for a pure OHSC fluid [12,14,32]. In contrast, the spherical particles aggregate in a dense phase that is above the fluid-crystalline phase transition in the monocomponent HS fluid [53]. Because of the lack of spatial order considerations in the PL theory, these numerical results should be considered with caution. In any case, the crystallisation of spherical particles induced by the discotic depleting agent has been reported in the past [34,37].

In the small spheres limit, the spherical particles act now as depleting agent favouring the aggregation of the discotic particles. In this case, the PL theory presents the same limitation because the predicted packing fraction of the discotic-rich phase is above the transition value to a more ordered phase such as the nematic or columnar. Consequently, the numerical result should be again considered with caution. In order to check if at least the qualitative predictions are valid, we have carried out MC–*NPT* computer simulations in the conditions where the PL approach predicts the demixing. In these simulations, initial configurations with low particle density and with all the particles at random positions and orientations were chosen. Then, a pressure which according to the PL theory produces a coexistence between nearly monocomponent phases was applied in a very long MC–*NPT* simulation. In Figure 3, an example of the states obtained by applying this procedure is shown. Results from the OHSC–HS fluid with $L^* = 0.05$ and $D_s^* = 0.1$ at pressure $P^* = 2000$ is presented. Under these conditions, PL theory predicts a coexistence between two states with $(x_v, \eta) = (0.89 \times 10^{-2}, 0.595)$ and (0.9999, 0.28). In the snapshot shown in Figure 3, the trend of the discotic particles to stack in simples columns surrounded by a diluted fluid of spherical particles, is observed. This is coherent with the prediction of the PL theory, the coexistence between a diluted sphere-rich state with a very packed and almost monocomponent fluid of discotic particles. As the PL theory does not consider spatial correlations, the formation of the columns is not predicted. In any case, the packing fraction predicted for the discotic rich state corresponds to columnar phases in the discotic monocomponent fluid [14]. It should be stressed that in this simulation, we are not using unphysical moves such as cluster moves or similar. For this reason, the coalescence of different columns would need of very long simulations. But it could be imagined that, in coherence with the results here discussed, the presence of small spherical particles could promote the formation of long columns or, in other words, nanowires. To the best of our knowledge, this is the first time that this prediction has been done. In any case, the confirmation of the details of this exciting phenomenon needs further research.

3.2. *Isotropic–nematic transition and equation of state*

In this section, the predictions obtained for the isotropic-to-nematic coexistence and the equations of state for both phases will be discussed. Hence, the dependence of the packing fraction η with molar fraction of spheres x_s at IN coexistence is shown in both panels of Figure 4. The particular cases of $L^* = 0.1$ (top panel) and $L^* = 0.05$ (bottom

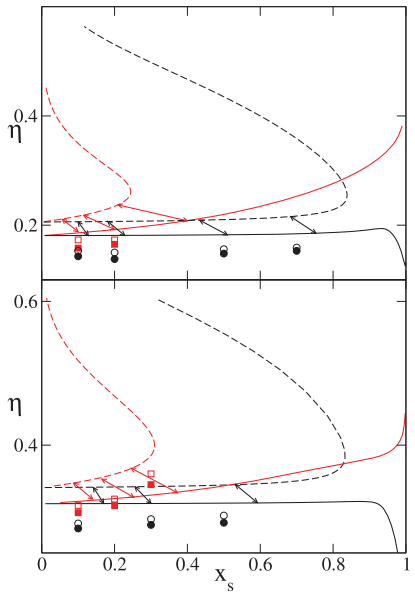

Figure 4. Dependence of the packing fraction with the molar fraction of spheres at the I–N coexistence as calculated by theory (solid lines) and limits of the stability of the isotropic and nematic phase found by simulations (symbols), for OHSC–HS fluids with $L^* = 0.05$ (top panel) and $L^* = 0.1$ (bottom panel). $D_s^* = 0.1$ (lower lines and circles) and 0.3 (upper lines and squares). Solid lines (theory) and solid symbols (simulation) correspond to the isotropic branch of the coexistence, while dashed lines and open symbols are the results for the nematic branch. In both panels, the upper curves of each type correspond to $D_s^* = 0.3$. Tie lines joining some coexisting states calculated by theory are included for illustration.

panel) with $D_s^* = 0.1$ and 0.3 are chosen to illustrate the general behaviour of the different molecular geometries and to compare them with simulation results. A general inspection of Figure 4, in combination with the dependence of the pressure at coexistence with x_s (not shown), reveals the existence of two different coexistence regimes, depending on the composition of the mixture. Few tie lines joining coexisting states calculated by theory have been added to facilitate the interpretation of the figure. At low values of x_s, the compositions in the isotropic and nematic phases are very similar, with packing fractions at coexistence close to the pure OHSC fluid. When x_s in the isotropic phase is increased, the difference in composition between the I and N phases also grows. This leads to a turning point, from where further increases on the fraction of spheres in the isotropic phase lead to a decrease on the amount of spheres in the nematic phase. Hence, beyond this turning point the mixture enters in a demixed regime, where a sphere-rich isotropic phase is in coexistence with a discotic-rich nematic phase. This global behaviour is similar to the described in the HSC–HS fluid [22]. For a given geometry of the discotic particles, the value of x_s where the turning point appears in the nematic branch is highly dependent on the diameter of the spherical particles. For both cases shown in Figure 4, it is possible to check that for $D_s^* = 0.1$, the phase separation is only found when the isotropic phase is very rich in spherical particles ($x_s \approx 0.8$). In contrast, for mixtures with bigger spherical particles, the turning point in the nematic branch of the coexistence appears for not very high values of x_s in this phase. There are also differences in the qualitative evolution of the packing fraction in the isotropic phase. For small spheres, in the isotropic branch of the coexistence, there is a decrease of the packing fraction there where x_s is high enough. In contrast, for bigger spheres, the packing fraction in the isotropic phase is always growing.

In order to check the validity of the Parsons–Lee theory described in this paper, computer simulation results are also presented in Figure 4. For all the cases shown in this figure, the computer results have the same qualitative behaviour than the theoretical values. In any case, the theory predicts that, at a given composition, the coexistence occurs at higher packing fractions that those found by computer simulation. It is also remarkable that for computer simulation results, the difference between the packing fraction in the isotropic and nematic phase is much lower than the theoretical predictions. This disagreement between PL and computer simulation results is bigger than the obtained in the equivalent comparison for the HSC–HS fluid. Two possible reasons could explain these differences away. First, the computer simulation results correspond to the limits of stability of the nematic phase. Hence, these points represent – at a given x_s – the last stable nematic and the first isotropic states found. This methodology leads to the possibility that the transitions from the nematic to the isotropic found by computer simulation were from a metastable state, and the packing fraction in the nematic phase was underestimated. In other words, the simulation points could be closer to the I–N spinodal than to the binodal curve. Moreover, it should be considered an intrinsic limitation of the Parsons–Lee theories for discotic particles. These theories are a refinement of the Onsager theory as we mentioned above. Onsager pointed out in his seminal paper that, in contrast with rod-like particles, the virial coefficients higher than the second can no longer be neglected for platelet particles [31]. So, the Parsons–Lee formalism is more inaccurate for the description of quantitative properties of the OHSC–HS fluid than in the HSC–HS case. With these considerations, the comparison between theory and simulations showed in Figure 4 presents an acceptable level of agreement from a qualitative point of view.

To extend the discussion of the PL theory predictions about the I–N transition in the HS-OHSC fluid, we show in Figures 5 and 6 the results for several particles sizes. Figure 5 summarises the results for OHSC–HS fluid with $L^* = 0.1$ and $D_s^* = 0.1$, 0.15, 0.2 and 0.3. In Figure 6, the results for discotic particles with $L^* = 0.05$ and spherical

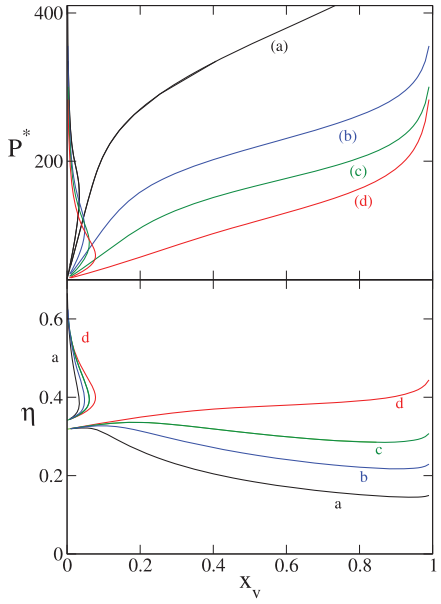

Figure 5. Dependence of the pressure $P^* = \beta P/D^3$ (top panel) and the packing fraction (bottom panel) with the volume fraction of spheres x_v at the isotropic-to-nematic coexistence predicted by PL theory for OHSC–HS fluids with (a) $L^* = 0.1$ and $D_s = 0.1$; (b) $L^* = 0.1$ and $D_s = 0.15$; (c) $L^* = 0.1$ and $D_s = 0.2$ and (d) $L^* = 0.1$ and $D_s = 0.3$.

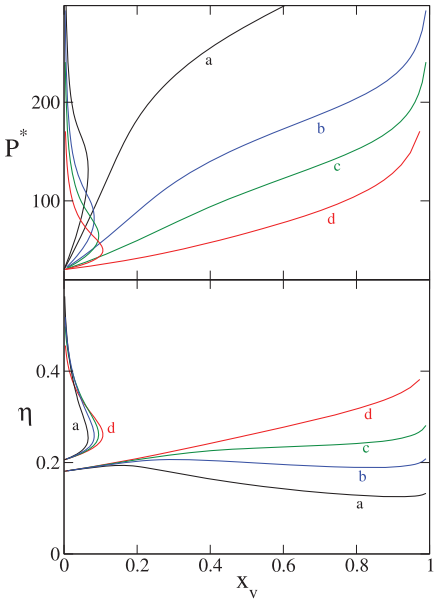

Figure 6. Same as Figure 5 but for $L^* = 0.05$.

particles with the same diameters than in Figure 5 are shown. In both figures, the dependence of the pressure in reduced units (top panel) and the packing fraction (lower panel) with the volumetric fraction of spheres x_v are presented. By means of the combined inspection of both panels, the pressure, packing fraction and composition of coexisting states can be determined. In both figures, we can observe the general characteristics described previously: in fluids with low concentration of spheres, there is coexistence between isotropic and nematic phase with little anisotropy in the composition. When the volume fraction of spheres in the isotropic phases is incremented, a turning point is reached and x_v in the nematic phase starts to decrease. For $L^* = 0.1$ and spheres with $D_s^* = 0.1$, an increment of x_v in the isotropic phase has as consequence a fast pressure growth at coexistence (top panel). On the other hand, the packing fraction (lower panel) clearly decreases in the isotropic phase when x_v is increased in this branch of the coexistence. In the nematic branch of the coexistence, the packing fraction grows monotonously with the value of x_v in the isotropic branch. This leads to a very asymmetric coexistence, between a diluted isotropic phase rich in spheres, and a concentrated nematic phase rich in discotic particles. This general qualitative behaviour is found for all the spherical diameters studied in this work. In any case, depending on the diameter of the spheres, there are important quantitative differences. Hence, an increase on the diameter of spheres has as consequence an important decrease of the pressure at coexistence for a given composition. It should be stressed that there is a strong relation between the decrease of the pressure at coexistence and the chosen reduced units. If the reduction $P^* = \beta P D_s^3$ were used, an increase of the pressure when the diameter of the spheres grows would be found. In any case, when the spheres' diameter grows the relation P^*/P^*_{OHSC} decreases; where P^*_{OHSC} is the pressure at coexistence for the OHSC monocomponent fluid. The change of the diameter of the spheres has two relevant consequences for the η value of the I–N phase diagram. First, in the isotropic branch η has a positive correlation with D_s^* at a given value of x_v. Besides, the dependence of the packing fraction in the isotropic branch with x_v also depends on D_s^*. Hence, when D_s^* grows, η changes in the isotropic phase from decreasing along with x_v for $D_s^* = 0.1$, to an almost constant value for $D_s^* = 0.15$ and growth for $D_s^* = 0.2$ and 0.3. In the nematic phase of the coexistence, the most relevant effect of the increment of D_s^* is the displacement of the turning point to higher values of x_v. The I–N phase diagram at $L^* = 0.05$ (Figure 6) shows the same characteristics. The main difference is the displacement of the I–N transitions up to higher pressures and lower packing fractions. To close the discussion about the effect of the addition of spheres in the liquid-crystal phase diagram of OHSC, it is interesting to note that, for situations where the nematic phase is stable in the monocomponent fluid of OHSC particles, the addition of spheres tends to destabilise the nematic phase. In all the cases studied in this work, the theory predicts

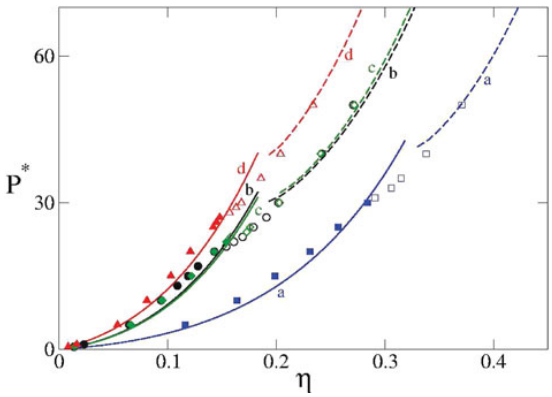

Figure 7. Equations of state at constant composition (isopleths) predicted by the Parsons–Lee theory (solid lines for isotropic and dashed lines for nematic branches, respectively) and obtained by computer simulation (solid symbols for isotropic and open symbols for nematic states) for OHSC–HS fluids with (L^*, D_s^*, x_s) = (0.05,0.1,0.1) (a, lines and circles); (0.1,0.1,0.1) (b, lines and squares); (0.05,0.3,0.1) (c, lines and diamonds) and (0.05,0.1,0.5) (d, lines and triangles). The pressure is reduced as in Figure 5.

that, when the volume fraction of spheres is incremented, the nematic phase is stable at higher values of the pressure and the packing fraction. This effect is the same that the found in the HSC–HS fluid. Most of the effects reported up to now, such as I-I demixing or broadening of the I-N binodals, have been also reported in another kind of mixtures, such mixtures of rod-like and spherical particles [22,54], or mixtures of platelets with non-adsorbing polymers [38,55]. As commented in the Introduction, to the best of our knowledge this is the first time that this rich phenomenology has been reported for the OHSC–HS fluid employing theory and simulation.

Finally, the prediction of the equation of states from PL theory and the comparison of this results with the obtained from Monte Carlo simulations is discussed and summarised in Figure 7. Hence, in Figure 7 the effect of the characteristics of the particles and the composition on the equation of state is shown. The Parsons–Lee equations of state at constant mixture composition (isopleths) for OHSC–HS mixtures are calculated for the L^* and HS diameters ranges where I–N transition occurs (mainly $L^* = 0.01$ and 0.05, D_s^* covering 0.1 and 0.3). The range of volume (or molar) fractions of HS considered in each case corresponds to the region of relatively small composition asymmetry in the coexisting I–N spinodals diagram calculated previously. This region lies before the entrance of the system into the demixed regime and is sufficiently anticipated with respect to the region where columnar phases may become relevant. The different isopleths show the expected positive correlation between pressure and packing fraction. For $L^* = 0.05$ and $D_s^* = 0.1$, an increment of x_s from 0.1 to 0.5 leads to an increment of the pressure at a given packing fraction in both I and N phases. This effect is related with the decrease of the average volume of the mixture v_m. The opposite effect is observed as the diameter of the spheres is increased at constant value of L^* and x_s. Figure 7 shows as the PL theory predicts, for $L^* = 0.05$ and $x_s = 0.1$ and a given value of η, that the fluid with $D_s^* = 0.3$ has lower pressure than for $D_s^* = 0.1$. This trend becomes smoother than the observed when x_s is changed. This smoothing for size ranges where the HS and HSC molecular volumes become comparable is a consequence of the effective compensation of the excluded volume contributions that drives the system pressure. However, such steric effects vary significantly from the isotropic to the nematic phase. Hence, for $L^* = 0.01$, $D_s^* = 0.3$, in the nematic phase, the trend observed in the isotropic phase is inverted. Similar conclusions could be extracted from the important reduction of the pressure at a given packing fraction when L^* changes from 0.05 to 0.1, fixing $x_s = 0.1$ and $D_s^* = 0.1$. Again, this could be related with the change in the relative volume occupied by the particles. Another effect is the displacement of the I–N transition towards greater packing values with growing molar fraction of HS due to the destabilisation of the nematic phase provoked by the depletion effects induced by the spherical component.

Isopleths for the isotropic and nematic phases have been reported here from MC–*NPT* simulations. The calculated points are included in Figure 7 as illustration of the qualitative agreement observed between the Parsons–Lee isopleths in the isotropic and nematic phases and the results from MC–*NPT* simulations for some particular cases. Here it is observed that, at a given packing fraction, the wider is the diameter of the spherical particles the higher is the pressure and the lower when the system is richer in spheres or for discotic particles with larger value for L^*. In any case, the numerical agreement between theory and simulation in all the cases shown in Figure 7 is not quantitatively accurate. It can be observed that, at given packing fraction, the values of P^* obtained by computer simulation are slightly larger than those predicted by the PL theory. This small but clear disagreement between theoretical and simulation results appears in both isotropic and nematic phases. This is in contrast with the very good agreement between the PL theory and computer simulation found in the fluid of hard prolate spherocylinders and hard spheres [22]. A similar level of inaccuracy for theories derived from Onsager's theories in systems with discotic particles has been reported by other authors in the past [42,43]. In contrast to fluids with prolate particles, where theoretical approaches give a good description of the model in both the immediacy of the isotropic-nematic transition and in the nematic phase itself, it gives a worse agreement between theory and simulation for discotic particles. This is a consequence of the intrinsic limitations of the theories based on Onsager's ideas to manage orientational order in discotic particles as it was commented above.

4. Conclusions and final remarks

The extension of the Parsons–Lee theory to the isotropic and nematic phase and the transition between them in binary mixtures of oblate hard spherocylinders and hard spheres have been discussed in detail. The results obtained within this approach have been checked with computer simulation results obtained in the *NPT* ensemble. In general, the qualitative concordance between theory and simulation is good for all the cases studied in this work. However, there are some numerical discrepancies and, hence, some of the results presented should be considered cautiously. The first disparity found in some of the results discussed is the appearance of IN transition packing fractions above the transition to columnar phases in the monocomponent OHSC fluid. The spatially structured phases are out of the scope of the PL theory. This could be more relevant in the study of the isotropic–isotropic demixing, where in some cases a coexistence of a very high packed and discotic-rich phase with another sphere-rich phase has been predicted. In any case, the computer simulation results confirm this coexistence, although between a isotropic fluid and cluster in columnar arrangement. These results could open the possibility of the stabilisation of nanowires by a spherical depleting agent. This exciting topic needs further research and will be the subject of a comprehensive report in the future.

On the other hand, this work confirms the limitations of the theories derived from Onsager's ideas for an accurate numerical description of systems containing discotic particles. A possible improvement route of the PL theory proposed here is a virial rescaling of the nematic phase with an appropriate reference system such as that proposed by Vega and Lago [56]. In relation to this improvement, a recent a theoretical study about the equation of state of monocomponent discotic particles including negative contributions to the virial expansion has been reported [44]. In this study, a generic equation of state for monocomponent discotic fluids with a higher agreement with simulation results that could be easily extended to multicomponent fluids, is proposed. This constitutes a promising approach towards the refinement of the results reported in this work.

Acknowledgements

Funding is acknowledged from the Operative Programme FEDER-Andalucia 2007–2013 through project P09-FQM-4938 and from Spanish Ministry of Science and Innovation (MICINN) through project MAT2011-29464.

References

[1] A. Grzybowski, C.E. Wilmer, J. Kim, K.P. Browne, and K.J.M. Bishop, Soft Matter **5**, 1110 (2009).
[2] S. Laschat, A. Baro, N. Steinke, F. Giesselmann, C. Hagele, G. Scalia, R. Judele, E. Kapatsina, S. Sauer, A. Schreivogel, and M. Tosoni, Angew. Chem. Int. Ed. **46**, 4832 (2007).
[3] I.W. Hamley, Angew. Chem. Int. Ed. **42**, 1692 (2003).
[4] S. Kumar, Chem. Soc. Rev. **35**, 83 (2006).
[5] L. Schmidt-Mende, A. Fechtenkotter, K. Mullen, E. Moons, R.H. Friend, and J.D. MacKenzie, Science **293**, 1119–1122 (2001).
[6] K.L. Woon, M.P. Aldred, P. Vlachos, G.H. Mehl, T. Stirner, S.M. Kelly, and M. O'Neill, Chem. Mater. **18**, 2311 (2006).
[7] K. Kawata, Chem. Rec. **2**, 59 (2002).
[8] M. Okazaki, K. Kawata, H. Nishikawa, and M. Negoro, Polym. Adv. Technol. **11**, 398 (2001).
[9] G.G. Nair, D.S.S. Rao, S.K. Prasad, S. Chandrasekhar, and S. Kumar, Mol. Cryst. Liq. Cryst. **397**, 245 (2003).
[10] S.C. McGrother, D.C. Williamson, and G. Jackson, J. Chem. Phys. **104**, 6755 (1996).
[11] P. Bolhuis and D. Frenkel, J. Chem. Phys. **101**, 666 (1997).
[12] B. Martínez-Haya and A. Cuetos, Mol. Simul. **35**, 1077 (2009).
[13] B. Martínez-Haya and A. Cuetos, Phys. Rev. **E 81**, 020701 (2010).
[14] M. Marechal, A. Cuetos, B. Martínez-Haya, and M. Dijkstra, J. Chem. Phys. **134**, 094501 (2011).
[15] F.M. van der Kooij and H.N.W. Lekkerkerker, Phys. Rev. Lett. **84**, 781 (2000).
[16] J.M. Brader, A. Esztermann, and M. Schmidt, Phys. Rev. **E 66**, 031401 (2002).
[17] P. Bolhuis, J. Brader, and M. Schmidt, J. Phys.: Condens. Matter **15**, S3421 (2003).
[18] Z. Dogic, K.R. Purdy, E. Grelet, M. Adams, and S. Fraden, Phys. Rev. **E 69**, 051702 (2004).
[19] S.V. Savenko and M. Dijkstra, J. Chem. Phys. **124**, 234902 (2006).
[20] S. Jungblut, R. Tuinier, K. Binder, and T. Schilling, J. Chem. Phys. **127**, 244909 (2007).
[21] G. Cinacchi, Y. Martinez-Raton, L. Mederos, G. Navascues, A. Tani, and E. Velasco, J. Chem. Phys. **127**, 214501 (2007).
[22] A. Cuetos, B. Martínez-Haya, S. Lago, and L. F. Rull, Phys. Rev. **E 75**, 061701 (2007).
[23] D. Kleshchanok, J.-M. Meijer, A.V. Petukhov, G. Portale, and H.N.W. Lekkerkekrker, Soft Matter **8**, 191 (2012).
[24] S. Asakura and F. Oosawa, J. Polym Sci. **32**, 183 (1958).
[25] T. Koda, M. Numajiri, and S. Ikeda, J. Phys. Soc. Jpn. **65**, 3551 (1996).
[26] A. Galindo, A.J. Haslam, S. Varga, G. Jackson, A.G. Vanakaras, D.J. Photinos, and D.A. Dunmur, J. Chem. Phys. **119**, 5216 (2003).
[27] A. Malijevsky, G. Jackson, and S. Varga, J. Chem. Phys. **129**, 144504 (2008).
[28] S. Belli, M. Dijkstra, and R. van Roij, J. Phys.: Condens. Matter **24**, 284128 (2012).
[29] A. Cuetos, A. Galindo, and G. Jackson, Phys. Rev. Lett **101**, 237802 (2008).
[30] J.P. O'Connell and J.M. Haile, *Thermodynamics: Fundamental for Applications* (Cambridge University Press, New York, 2005).
[31] L. Onsager, Ann. N.Y. Acad. Sci. **51**, 627 (1949).
[32] A. Cuetos and B. Martínez-Haya, J. Chem. Phys. **129**, 214706 (2008).
[33] B. Martínez-Haya and A. Cuetos, J. Chem. Phys. **131**, 074901 (2009).
[34] S.M. Oversteegen and H.N.W. Lekkerkerker, J. Chem. Phys., **120**, 2470 (2004).
[35] L. Harnau and S. Dietrich, Phys. Rew. **E 69**, 051501 (2004).
[36] D.J. Voorn, W. Ming, J. Lavenb, J. Meuldijk, G. de With, and A.M. van Herk, Colloids Surf., **A 294**, 236246 (2007).
[37] N. Doshi, G. Cinacchi, J.S. van Duijneveldt, T. Cosgrove, S.W. Prescott, I. Grillo, J. Phipps, and D.I. Gittins, J. Phys.: Condens. Matter **23**, 194109 (2011).

[38] S.-D. Zhang, P.A. Reynolds, and J.S. van Duijneveldt, J. Chem. Phys. **117**, 9947 (2002).
[39] D. Kleshchanok, J.-M. Meijer, A.V. Petukhov, G. Portale, and H.N.W. Lekkerkerker, Soft Matter **8**, 191–197 (2012).
[40] J.D. Parsons, Phys. Rev. **A 19**, 1225 (1979).
[41] S.D. Lee, J. Chem. Phys. **87**, 4972 (1987).
[42] F. Gámez, P.J. Merkling, and S. Lago, Chem. Phys. Lett. **494**, 45–49 (2010).
[43] H.H. Wensink and H.N.W. Lekkerkerker, Mol. Phys. **107**, 2111–2118 (2009).
[44] L. Wu, H.H. Wensink, G. Jackson, and E.A. Müller, Mol. Phys. **110**, 1269–1288 (2012).
[45] Y. Rosenfeld, Phys. Rev. Lett. **63**, 980 (1989).
[46] A. Esztermann, H. Reich, and M. Schmidt, Phys. Rev. **E 73**, 011409 (2006).
[47] J.A. Capitán, Y. Martínez–Ratón, and J.A. Cuesta, J. Chem. Phys. **128**, 194901-8 (2008).
[48] Y. Martínez–Ratón and J.A. Cuesta, Mol. Phys. **107** 4–6, 415–422 (2009).
[49] N.F. Carnahan and K.E. Starling, J. Chem. Phys. **51**, 635–636 (1969).
[50] B. Mulder, Mol. Phys. **103**, 113 (2005).
[51] R. van Roij and B. Mulder, Phys. Rev. **E 54**, 6430 (1996).
[52] R. Eppenga and D. Frenkel, Mol. Phys. **52**, 1303 (1984).
[53] W.G. Hoover and F.H. Ree, J. Chem. Phys. **49**, 3609 (1968).
[54] S. Lago, A. Cuetos, B. Martínez–Haya, and L.F. Rull, J. Mol. Recognit. **17**, 417 (2004).
[55] V.V. Ginzburg and A.C. Balazs, Macromolecules **32**, 5681 (1999).
[56] C. Vega and S. Lago, J. Chem. Phys. **100**, 6727 (1994).